

# Electrophysiological and Behavioral Evidence of Reduced Binaural Temporal Processing in the Aging and Hearing Impaired Human Auditory System

Trends in Hearing  
Volume 22: 1–12  
© The Author(s) 2018  
Reprints and permissions:  
sagepub.co.uk/journalsPermissions.nav  
DOI: 10.1177/2331216518785733  
journals.sagepub.com/home/tia  


Charlotte Vercammen<sup>1</sup> , Tine Goossens<sup>1</sup>, Jaime Undurraga<sup>2,3</sup>,  
Jan Wouters<sup>1</sup>, and Astrid van Wieringen<sup>1</sup>

## Abstract

A person's ability to process temporal fine structure information is indispensable for speech understanding. As speech understanding typically deteriorates throughout adult life, this study aimed to disentangle age and hearing impairment (HI)-related changes in binaural temporal processing. This was achieved by examining neural and behavioral processing of interaural phase differences (IPDs). Neural IPD processing was studied electrophysiologically through steady-state activity in the electroencephalogram evoked by periodic changes in IPDs over time, embedded in the temporal fine structure of acoustic stimulation. In addition, behavioral IPD discrimination thresholds were determined for the same stimuli. To disentangle potential effects of age from those of HI, both measures were applied to six participant groups: young, middle-aged, and older persons, with either normal hearing or sensorineural HI. All participants passed a cognitive screening, and stimulus audibility was controlled for in participants with HI. The results demonstrated that HI changes neural processing of binaural temporal information for all age-groups included in this study. These outcomes were revealed, superimposed on age-related changes that emerge between young adulthood and middle age. Poorer neural outcomes were also associated with poorer behavioral performance, even though the behavioral IPD discrimination thresholds were affected by age rather than by HI. The neural outcomes of this study are the first to evidence and disentangle the dual load of age and HI on binaural temporal processing. These results could be a valuable first step toward future research on rehabilitation.

## Keywords

humans, adult, hearing loss, auditory evoked potentials, electroencephalography

Date received: 8 February 2018; accepted: 4 June 2018

## Introduction

With advancing age, our ability to understand speech in noise deteriorates. This is, in part, mediated by changes in peripheral hearing sensitivity (CHABA, 1988; Gates & Mills, 2005). In addition, age and hearing impairment (HI) affect cognitive skills as well as the ability to encode temporal information (CHABA, 1988; Gates & Mills, 2005) conveyed in the envelope and temporal fine structure (TFS) of acoustic waveforms (Moore, 2014). Adequate processing of both envelope and TFS information is indispensable for speech understanding (Swaminathan & Heinz, 2012; Zeng et al., 2005). Moreover, binaural TFS processing underlies spatial release from masking, that is, a binaural advantage that results in improved speech understanding when a

speech target is spatially separated from interfering sound streams (Swaminathan et al., 2016). This study was designed to gain more insight in age- and HI-related changes in binaural TFS processing throughout adult life.

<sup>1</sup>Department of Neurosciences, Research Group Experimental Oto-Rhino-Laryngology, KU Leuven—University of Leuven, Belgium

<sup>2</sup>Department of Linguistics, The Australian Hearing Hub, Macquarie University, Sydney, Australia

<sup>3</sup>Ear Institute, University College London, London, UK

## Corresponding Author:

Charlotte Vercammen, Department of Neurosciences, Research Group Experimental Oto-Rhino-Laryngology, KU Leuven—University of Leuven, Onderwijs en Navorsing 2, Herestraat 49 Bus 721, 3000 Leuven, Belgium.  
Email: Charlotte.Vercammen@kuleuven.be



Neural encoding of TFS information relies on phase-locking, as hair cells induce action potentials in postsynaptic auditory nerve fibers synchronized to a particular part of a periodic acoustic waveform (Heil & Peterson, 2015; Rose, Brugge, Anderson, & Hind, 1967). Neural encoded TFS information is exchanged between the left and right auditory pathways in the superior olivary complex. This exchange allows the extraction of binaural information (Remme et al., 2014), such as interaural differences in timing (ITDs) or phase (IPDs; with IPDs the equivalent of ITDs for ongoing, periodic stimuli). As age and HI are associated with low-level neurodegeneration of the auditory nerve (Makary, Shin, Kujawa, Liberman, & Merchant, 2011; McFadden, Ding, Jiang, & Salvi, 2004; Sergeenko, Lall, Liberman, & Kujawa, 2013; Spoendlin, 1975), both are likely to affect TFS encoding at subsequent stages of the auditory system. In addition, age and HI are associated with neurochemical changes in inhibitory neurotransmitter release. This mechanism elicits increased spontaneous neural activity (Caspary, Ling, Turner, & Hughes, 2008) that could increase the amount of jitter on binaural neural transmission, thereby reducing phase-locking in binaural cells and interfering with temporal encoding as well.

Different behavioral and physiological studies in adult listeners confirm that age affects IPD processing, that is, the ability to process changes in IPDs over time (Füllgrabe, 2013; Hopkins & Moore, 2011; Papesh, Folmer, & Gallun, 2017; Ross, Fujioka, Tremblay, & Picton, 2007; Tremblay, Picton, & Ross, 2007). However, it is unclear whether HI affects IPD processing in addition to age. To our knowledge, only one behavioral study demonstrates an association between hearing thresholds and low-frequency IPD processing (King, Hopkins, & Plack, 2014), but it contradicts earlier findings (Hopkins & Moore, 2011; Lacher-Fougère & Demany, 2005; Moore, Glasberg, Stoev, Füllgrabe, & Hopkins, 2012; Strelcyk & Dau, 2009). Also, physiological studies that demonstrate how advancing age yields reduced cortical IPD processing (Papesh et al., 2017; Ross et al., 2007; Tremblay et al., 2007) were not able to tease out contributions of high-frequency HI. Due to the importance of IPD processing for speech understanding in multitalker situations (Oberfeld & Klöckner-Nowotny, 2016), the need has emerged to disentangle detrimental effects of age from HI on changes in binaural temporal processing in adult listeners. To this end, this study examined neural and behavioral IPD processing in six participant groups: young, middle-aged, and older participants, with either normal hearing (NH) thresholds or sensorineural HI (i.e., originating at cochlear or neural level). Neural IPD processing was studied electrophysiologically using a recently developed measure that records neural responses to periodic changes in IPDs over time, embedded in the TFS of

acoustic stimuli (Haywood, Undurraga, Marquardt, & McAlpine, 2015; McAlpine, Haywood, Undurraga, & Marquardt, 2016; Undurraga, Haywood, Marquardt, & McAlpine, 2016). In addition, behavioral IPD processing was examined through IPD discrimination thresholds, obtained for similar stimuli as those applied during the electrophysiological measurements. It was expected that both the neural and behavioral outcomes would change as a function of advancing age (Füllgrabe, 2013; Hopkins & Moore, 2011; Papesh et al., 2017; Ross et al., 2007; Tremblay et al., 2007). A lack of physiological studies regarding potential contributions of HI to changes in IPD processing, as well as contradictory behavioral outcomes regarding this topic, motivated this study to disentangle potential HI-related from age-related changes in binaural temporal processing. All participants included in this study passed a cognitive screening, and stimulus audibility was controlled for in participants with HI.

## Materials and Methods

### Participants

Young, middle-aged, and older participants with NH and with sensorineural HI were recruited, resulting in six participant groups (see Table 1). Pure-tone audiometric thresholds at octave frequencies from 125 to 8000 Hz were determined for both ears separately in a soundproof booth, by means of the Hughson Westlake 5-up 10-down procedure (Carhart & Jerger, 1959), a Madsen OB922 clinical audiometer, and TDH-39 earphones. Bone conduction thresholds were obtained at octave frequencies from 500 to 2000 Hz, by means of a RadioEar B71 bone transducer. NH was defined as pure-tone air conduction thresholds  $\leq 25$  dB HL at octave frequencies from 125 to 4000 Hz in both ears. HI was defined as pure-tone air conduction thresholds  $\geq 35$  dB HL at octave frequencies from 1000 to 8000 Hz in both ears (see Figure 1). All participants with HI had air bone gaps  $\leq 10$  dB HL, confirming the sensorineural nature of their HI. For all participants, the interaural difference in hearing thresholds near the stimulation frequency (500 Hz—see Auditory stimulation) did not exceed 10 dB HL. To minimize potential cognitive confounds (Lister et al., 2016), participants were only included when they scored  $\geq 26/30$  on the Montreal Cognitive Assessment (Nasreddine et al., 2005), a cognitive screening tool that is sensitive and specific to detect even mild cognitive impairments. None of the participants reported a known history of tinnitus, head trauma, or neurological problems.

The study was approved by the Medical Ethical Committee of the University Hospitals KU Leuven (approval no. B322201214866) and participants gave

**Table 1.** Participant Details.

	NH participants		Participants with HI	
	$n^a$ (women/men)	Med age $\pm$ IQR <sup>b</sup> (years)	$n^a$ (women/men)	Med age $\pm$ IQR <sup>b</sup> (years)
Young	10 (8/2)	22 $\pm$ 1	9 (6/3)	28 $\pm$ 4
Middle-aged	10 (7/3)	53 $\pm$ 4	11 (7/4)	60 $\pm$ 1
Older	8 (5/3)	72 $\pm$ 2	8 (4/4)	79 $\pm$ 3

Note. IQR = interquartile range; NH = normal hearing; HI = hearing impairment.

<sup>a</sup>Number of participants ( $n$ ), including the ratio of number of women to men.

<sup>b</sup>Median age  $\pm$  interquartile range per participant group (Med age  $\pm$  IQR) in years.

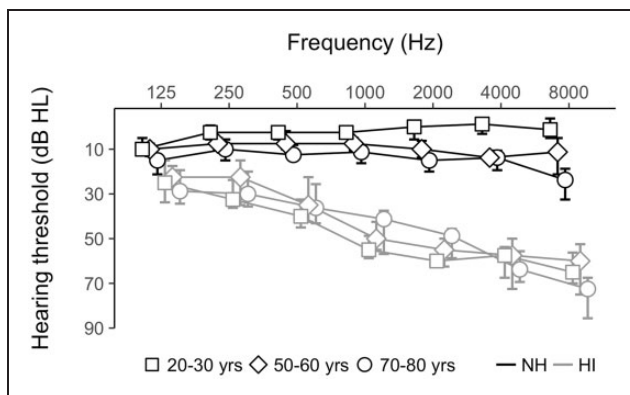


**Figure 1.** Pure-tone audiometry: median hearing thresholds with interquartile ranges in dB HL for the six participants groups. Black lines represent data of NH participants, gray lines data of participants with HI. Squares, diamonds, and circles correspond to data of young (20–30 years), middle-aged (50–60 years), and older participants (70–80 years), respectively.

NH = normal hearing; HI = hearing impairment.

written informed consent after being fully informed about the study.

### Interaural Phase Modulation—Following Response

Neural IPD processing was investigated electrophysiologically by means of interaural phase modulation—following responses (IPM-FRs; Haywood et al., 2015; McAlpine et al., 2016; Undurraga et al., 2016). The IPM-FRs were evoked by IPMs, that is, periodic changes in IPDs over time that were embedded in the TFS of acoustic stimulation. The amplitude of the IPM-FRs represents steady-state activity in the electroencephalogram (EEG), that is, the consistency of the neural activity in amplitude and phase over epochs (McAlpine et al., 2016). As the IPM-FR amplitudes correlated with behavioral IPD processing in young NH adults, Undurraga et al. (2016) demonstrated that the amplitudes are a

robust measure of neural IPD processing in this population.

**Auditory stimulation.** IPM-FRs were recorded in response to 100% sinusoidal amplitude modulated pure tones with a carrier frequency of 492 Hz and a modulation frequency of 82 Hz. The IPMs, embedded in the TFS of the carrier wave, introduced a periodic switch in the stimulation between a diotic (no IPD present) and a dichotic part (IPD present). The periodic switch was introduced every 0.17 seconds, which corresponded to a switch rate of 5.86 Hz (see Figure 2). In addition, the IPM depth was manipulated and 11 stimulus conditions were created, that is, stimuli with IPMs of 180°, 144°, 115°, 92°, 59°, 38°, 24°, 15°, 10°, 5°, and 0°. The IPMs were implemented symmetrically between the two ears, for example, an IPM depth of 180° was implemented as a phase shift of  $\pm 90^\circ$  in each ear (see Figure 2). Phase shifts were introduced at the minimum of the modulation cycle to prevent acoustic distortions (Haywood et al., 2015; Undurraga et al., 2016).

Stimuli were presented bilaterally using a laptop, custom written software, a Fireface Hammerfall DSP Multiface II external soundcard, and magnetically shielded ER-3A insert phones. The stimuli were presented at a fixed intensity of 65 dB SPL for NH participants. For participants with HI, the intensity was individually set to create a loudness sensation similar to that of their NH peers (see Behavioral loudness adjustment). Level calibration was performed by means of a Bruel and Kjaer sound level meter (type 2260), a ZC-0026 preamplifier, and a 2-cc coupler artificial ear (type 4152). The 11 stimulus conditions were all presented twice in blocks of 300 seconds. The order of conditions was randomized across participants.

**EEG recordings.** The EEG was recorded using a 64-channel BioSemi ActiveTwo system. Participants sat comfortably in a chair in a double-walled, soundproof, and electromagnetically shielded booth while they watched a silent movie of their choice with subtitles. The

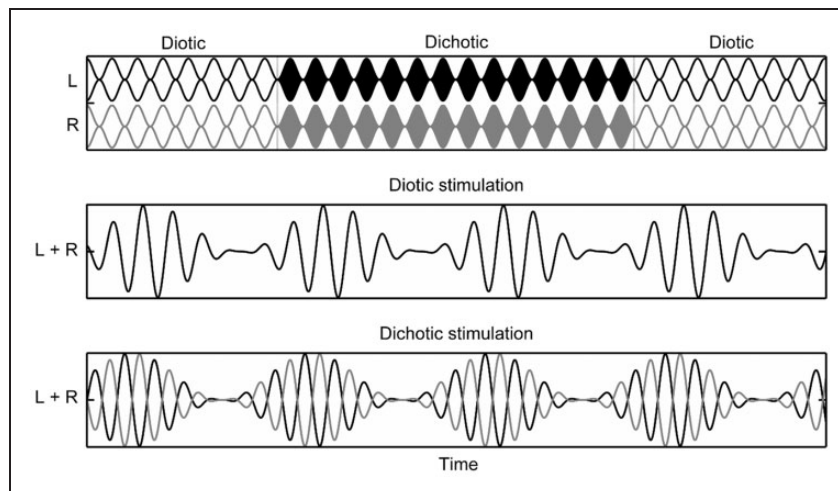


**Figure 2.** Schematic overview of the electrophysiological and behavioral stimuli, with a sinusoidal carrier wave of 492 Hz, 100% amplitude modulated at a rate of 82 Hz. The stimuli contain an IPM at a switch rate of 5.86 Hz, that is, an IPD change is introduced every 0.17 seconds, resulting in an alternation between diotic and dichotic stimulation. The IPD changes are indicated in the top panel of the figure by vertical lines. Solid black and gray areas represent dichotic stimulation, whereas empty areas represent diotic stimulation. Black signals are presented to the left ear (L) and gray signals to the right ear (R). The middle panel of the figure illustrates those parts of the stimulation that are diotic, that is, the signals in the left and right ear (L+R) are in phase. The bottom panel of the figure illustrates those parts of the stimulation that are dichotic, that is, the signals in the left and right ear (L+R) are shifted in phase relative to each other. In this example, the IPM depth is  $180^\circ$ . Therefore, the signals in the left and right ear are out of phase during dichotic stimulation. With decreasing IPM depth, the phase shifts between the signals in the left and right ear become smaller. Phase shifts are always introduced at the minimum of the modulation cycle to prevent acoustic distortions.

participants wore a head cap in which 64 active Ag-AgCl pin-type electrodes were mounted, according to the International 10/10 System (American Clinical Neurophysiology Society, 2006). Electrode offsets were kept stable and below 40 mV. The EEG signal was AD converted at a sampling rate of 8192 Hz and amplified by an ActiveTwo amplifier, with an incorporated low-pass filter with cutoff frequency of 1638 Hz. The EEG was visualized and stored by BioSemi ActiView software. Total measurement time was approximately 2 hours. A short break was introduced every 30 minutes.

**EEG processing.** EEG data were processed in Matlab R2013a (The MathWorks Inc., 2013) and referenced to Cz. EEG signals recorded by electrodes O1, O2, PO3, PO4, PO7, PO8, P5, P6, P7, P8, P9, P10, CP5, CP6, TP7, and TP8 were averaged in the time domain. This electrode selection was adopted from a previous study in our research group that included similar participant groups. The selection resulted from a data-driven approach and includes those electrodes that recorded the highest response amplitudes (Goossens, Vercammen, Wouters, & van Wieringen, 2016). Per participant and per IPD condition, the resulting EEG signal was segmented in epochs of approximately 1 second, based on triggers sent from the stimulation software in order to synchronize stimulation and recording. Per stimulus condition, epochs resulting from two recording

blocks of 300 seconds were concatenated and 5% of the epochs with the largest peak-to-peak amplitudes were rejected to remove artifacts. This resulted in 554 epochs per stimulus condition. Per epoch, a Fast Fourier Transform was performed to calculate the complex frequency spectrum, from which the response power, amplitude, and phase at the switch rate (5.86 Hz) were obtained. Mean response power, amplitude, and phase were the result of vector averaging across epochs. It is assumed that the average response at the switch rate is a combination of a steady-state response, with constant amplitude and phase over time, and background noise, with random amplitude and phase over time. Therefore, the background noise was estimated as the standard deviation (*SD*) of the mean response over epochs, divided by the square root of the number of epochs (Gransier, van Wieringen, & Wouters, 2017).

### **Behavioral IPD Discrimination Thresholds and Loudness Adjustment**

The behavioral tasks were performed in a soundproof booth by means of Apex software (Francart, van Wieringen, & Wouters, 2008), a Fireface Hammerfall DSP Multiface II external soundcard, and ER-3A insert phones.

**Behavioral IPD discrimination thresholds.** Behavioral IPD processing was investigated through IPD discrimination.

For every participant, behavioral IPD discrimination thresholds were estimated using a three alternative forced choice task, following an adaptive 2-down, 1-up procedure (Levitt, 1971). Per trial, participants listened to three 100% sinusoidal amplitude modulated pure tones with a carrier frequency of 492 Hz and a modulation frequency of 82 Hz. Two of three stimuli were static, that is, they did not contain an IPD. One stimulus was dynamic, that is, it switched between a diotic (no IPD) and a dichotic part (IPD present in the TFS of the carrier wave) over time, at a rate of 5.86 Hz. The dynamic stimuli were similar to those used in the IPM-FR procedure (see Figure 2). Phase shifts were introduced at the minimum of the modulation cycle to prevent acoustic distortions. Every stimulus lasted 1.4 seconds and subsequent stimuli were separated by 500 ms of silence. Participants were instructed to select the dynamic sound. At baseline, the IPM depth was 180°. Following two subsequent correct responses, the IPM depth decreased by a factor. Following an incorrect response, the IPD depth increased by a factor. The factor was 1.25<sup>3</sup> at baseline and reduced to 1.25<sup>2</sup> and 1.25 after one and three reversals, respectively. Visual feedback was provided after every trial and the task ended after eight reversals. The behavioral IPD discrimination threshold per participant was defined as the geometric mean of the IPM depths across the last six reversals. Participants performed the task 3 times. Similar to the electrophysiological measurements, stimulus intensity was 65 dB SPL for participants with NH and individually set based on subjective loudness sensation for participants with HI (as is explained in the following two paragraphs).

**Behavioral loudness categorization.** As a reference for the loudness adjustment procedure for participants with HI (explained in the following paragraph), the loudness of 65 dB SPL for NH participants was determined per age cohort, through a loudness categorization task. During the task, the intensity of the IPM-FR stimulus with an IPM depth of 180° (see Figure 2) was manipulated in steps of 10 dB, ranging from 45 to 85 dB SPL. Every intensity was presented 3 times. Participants were asked to select the position along a visual analog scale that corresponded to their subjective loudness sensation of every intensity. The visual analog scale consisted of a vertical line and seven marks, equidistant from each other, ranging from *inaudible* (bottom mark) over *very soft*, *soft*, *comfortable*, *loud*, *very loud*, to *uncomfortably loud* (upper mark). NH participants performed the loudness categorization task 3 times and as such, the loudness of 65 dB SPL was assessed 9 times per participant. Per participant, the arithmetic mean of the nine trials was determined, and per age cohort, the arithmetic mean of the loudness of 65 dB SPL across participants was determined and used as a reference for the behavioral

loudness adjustment procedure for participants with HI (see the following section).

**Behavioral loudness adjustment.** Participants with HI, in turn, were asked to adjust the sound pressure level by which the IPM-FR stimulus with an IPM depth of 180° (see Figure 2) was administered until it subjectively corresponded to a red cross on the visual analog scale, marking the mean loudness of 65 dB SPL for the corresponding NH age-group. Participants adjusted the sound pressure level using six buttons on the screen: +(1 dB), ++ (+3 dB), +++ (+5 dB) and -(1 dB), -- (-3 dB), --- (-5 dB). The participants were asked to perform the loudness adjustment procedure 4 times. The arithmetic means of the four resulting intensities determined the individual intensity setting for a particular participant, which was used during the electrophysiological and behavioral tasks. The resulting stimulation intensities ranged between 62 and 94 dB SPL for young, between 63 and 83 dB SPL for middle-aged, and between 63 and 78 dB SPL for older participants with HI.

### Statistical Analyses

Statistical analyses were performed in R (R Core Team, 2017) and SPSS Statistics 24 (IBM Corporation, 2016).

**Interaural phase modulation—Following response.** Linear mixed effect (LME) models (Baayen, Davidson, & Bates, 2008; Bates, Machler, Bolker, & Walker, 2015; Magezi, 2015; Koerner & Zhang, 2017) were applied to determine whether age and HI contributed to predicting the IPM-FR amplitudes at the switch rate, across IPM depths. Amplitude estimations of the background noise were investigated as well, as both IPM-FR and noise amplitudes determine the signal-to-noise ratio of neural responses. The LME models were fitted using the *lmer*-package (Kuznetsova, Brockhoff, & Christensen, 2016) for R (R Core Team, 2017).

The amplitudes of the IPM-FR and background noise estimations were square root transformed to meet the assumption of normality of residuals, as was confirmed by visual inspection and Shapiro–Wilk testing (IPM-FR:  $p = .14$ ; noise:  $p = .21$ ). Age-group (young, middle-aged, and older), hearing status (NH, HI), and IPM depth (from 0° to 180°) were added as fixed factors to the LME models, predicting either the IPM-FR amplitudes, or either the noise estimations. The factor Participants was entered into the models as a random factor. Factors that did not significantly contribute to the model were discarded by a backward stepwise reduction method and the contribution of each variable to predicting the responses was assessed at an  $\alpha$ -level of .05. The variance components of the random effects were estimated using restricted maximum likelihood estimation, and

Sattherwaite approximations estimated the degrees of freedom of the models.

**Behavioral IPD discrimination thresholds.** Potential effects of age and HI on behavioral IPD discrimination thresholds were investigated by means of an independent factorial analysis of variance. The dependent variable (behavioral IPD discrimination thresholds) was logarithmically transformed to meet the assumption of normality. Age-group (young, middle-aged, and older) and hearing status (NH, HI) were added to the model as two categorical independent variables. The analyses were two-tailed ( $\alpha = .05$ ).

For reasons of clarity, descriptive statistics concerning the behavioral IPD discrimination thresholds are reported and visualized in degrees in Table 2 and Figure 5. The mean IPD discrimination thresholds and their *SDs* were determined per cohort based on the logarithmically transformed values, after which they were transformed back to degrees.

**Relationship IPM-FR—Behavioral IPD discrimination thresholds.** Potential associations between the electrophysiological IPM-FR amplitudes and behavioral IPD discrimination thresholds were investigated through Spearman's rho correlation coefficients. To obtain one IPM-FR value per participant, the difference between the maximum and minimum IPM-FR amplitudes was determined across IPM depths and referred to as the dynamic range of the IPM-FR of that participant (in  $\mu\text{V}$ ).

**IPD processing and peripheral hearing sensitivity.** Care was taken to control peripheral hearing sensitivity in this study, by selecting participants with hearing thresholds  $\leq 25$  dB HL at octave frequencies from 125 to 4000 Hz (NH participants) or with hearing thresholds  $\geq 35$  dB HL at octave frequencies from 1000 to 8000 Hz

(participants with HI; see Figure 1). As participants with NH and HI belonged to three age cohorts, additional analyses were performed to determine whether age affected peripheral hearing sensitivity, despite the strict inclusion criteria. The carrier wave of the stimuli in this study was 492 Hz. Therefore, nonparametric Kruskal–Wallis tests ( $\alpha = .05$ ) were applied to pure-tone audiometric thresholds at 500 Hz across age cohorts. This was done separately for NH participants and for participants with HI.

## Results

### Interaural Phase Modulation—Following Response

Figure 3 shows typical examples of the IPM-FRs in the EEG frequency spectrum, for an IPM depth of  $180^\circ$ . Figure 4 shows the individual IPM-FRs of all participants as a function of IPM depth and the trends in the data through robust linear fits.

An LME model revealed that age-group,  $F(2, 52) = 12.36$ ,  $p < .001$ , hearing status,  $F(1, 52) = 4.35$ ,  $p = .04$ , IPM depth,  $F(1, 54) = 273.64$ ,  $p < .001$ , and an

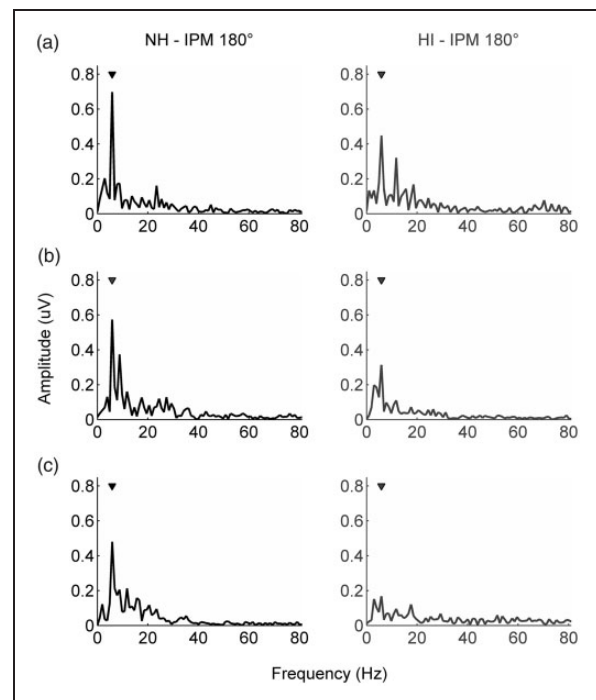


**Figure 3.** Typical examples of the IPM-FRs (y axis;  $\mu\text{V}$ ) in the EEG frequency spectrum (x axis; Hz) for an IPM depth of  $180^\circ$ . Typical examples are provided for young (a), middle-aged (b), and older participants (c), with NH (left column) and sensorineural HI (right column). Per typical example, the triangle indicates the IPM-FR, that is, the response at the switch rate (5.86 Hz). NH = normal hearing; HI = hearing impairment.

**Table 2.** Descriptive Statistics for the Behavioral IPD Discrimination Thresholds.

	NH participants		Participants with HI	
	$n^a$	$M$ (IPD) [ $SD$ (IPD)] <sup>b</sup>	$n^a$	$M$ (IPD) [ $SD$ (IPD)] <sup>b</sup>
Young	10	13 [1]	9	17 [2]
Middle-aged	10	18 [2]	10	23 [2]
Older	8	43 [2]	7	46 [2]

Note. IPD = interaural phase difference; SD = standard deviation; NH = normal hearing; HI = hearing impairment.

<sup>a</sup>Number of participants.

<sup>b</sup>Geometric mean IPD discrimination thresholds ( $^\circ$ ) [geometric standard deviation per cohort].

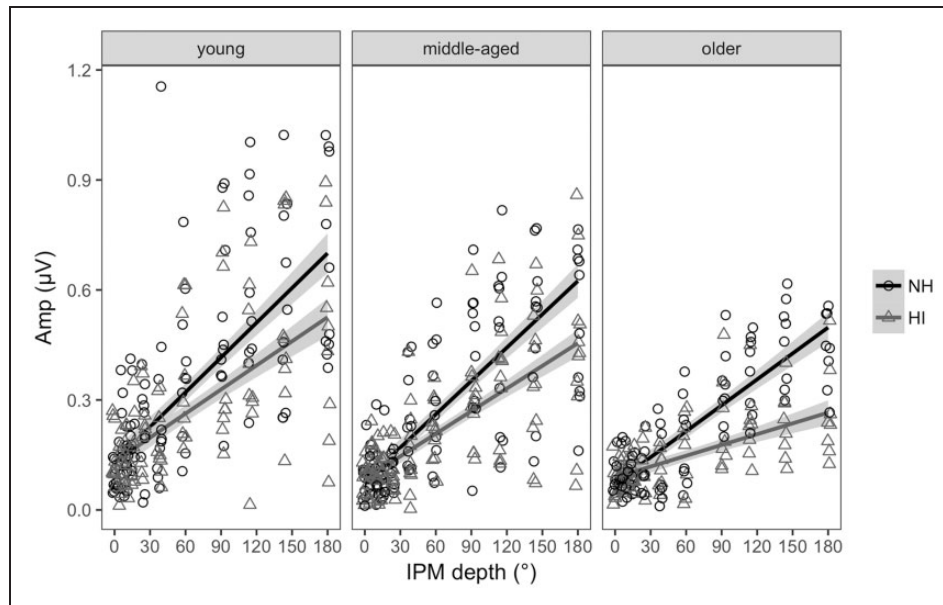


**Figure 4.** Individual data points represent the individual IPM-FR amplitudes of all participants across IPM depth ( $^{\circ}$ ). IPM depth ( $^{\circ}$ ) is visualized on the x axis and response amplitude ( $\mu\text{V}$ ) of the IPM-FRs on the y axis. Black circles correspond to data of NH participants and gray triangles to data of participants with HI. Black and gray lines represent robust linear fits of the IPM-FR amplitudes for, respectively, NH participants and participants with HI. Light gray shading visualizes the 95% confidence interval of the corresponding robust linear fits. The data are visualized, from left to right, for young, middle-aged, and older participants. IPM = interaural phase modulation; NH = normal hearing; HI = hearing impairment.

interaction effect between IPM depth and hearing status,  $F(1, 54) = 7.94$ ,  $p = .007$ , significantly contributed to predicting the IPM-FR amplitudes.

The main effect of age-group is reflected by the reduced steepness of the linear fit slopes with advancing age in Figure 4. Bonferroni-corrected post hoc tests revealed that the IPM-FR amplitudes were significantly lower for middle-aged, difference of least square means (LSM) =  $0.07 \mu\text{V}$ , standard error ( $SE$ ) =  $0.02 \mu\text{V}$ ,  $t(52.3) = 3.82$ ,  $p < .001$ , and older participants, LSM =  $0.09 \mu\text{V}$ ,  $SE = 0.02 \mu\text{V}$ ,  $t(52.2) = 4.70$ ,  $p < .001$ , compared with young participants. IPM-FR amplitudes did not significantly differ between middle-aged and older participants, LSM =  $0.02 \mu\text{V}$ ,  $SE = 0.02 \mu\text{V}$ ,  $t(51.8) = 1.15$ ,  $p = .25$ . The main effect of hearing status is reflected by the slopes of the linear fits as well (see Figure 4). The slopes of the linear fits are less steep for data of participants with HI compared with data of NH participants, irrespective of age-group. This reduced steepness of the slopes reflects overall lower IPM-FR amplitudes (in  $\mu\text{V}$ ) for participants with HI compared with NH participants (LSM =  $0.04 \mu\text{V}$ ,  $SE = 0.02 \mu\text{V}$ ). The LME model also demonstrated a significant main effect of IPM depth,  $F(1, 54) = 274$ ,  $p < .001$ , and an interaction effect between IPM depth and hearing status,  $F(1, 54) = 8$ ,  $p = .007$ . The IPM-FR amplitudes indeed increased with increasing IPM depth for all participant groups. Moreover, HI yielded a greater amplitude reduction for larger than

for smaller IPM depths for every age-group, especially above  $30^{\circ}$  (see Figure 4).

As both IPM-FR and noise amplitudes determine the signal-to-noise ratio of neural responses, an LME model was fitted to the noise amplitudes as well. The model showed that age was the only factor that contributed significantly to the model,  $F(2, 53) = 7$ ,  $p = .003$ . Bonferroni corrected post hoc tests showed that the noise amplitudes were significantly lower for middle aged compared with young participants, LSM =  $0.03 \mu\text{V}$ ,  $SE = 0.01 \mu\text{V}$ ,  $t(52.9) = 3.08$ ,  $p = .003$ , and for older compared with young participants, LSM =  $0.03 \mu\text{V}$ ,  $SE = 0.01 \mu\text{V}$ ,  $t(52.9) = 3.21$ ,  $p = .002$ , but not for older compared with middle-aged participants, LSM =  $0.003 \mu\text{V}$ ,  $SE = 0.01 \mu\text{V}$ ,  $t(52.9) = 0.35$ ,  $p = .73$ . Thereby, age affected the noise amplitudes (young–middle-aged: LSM =  $0.03 \mu\text{V}$ ,  $SE = 0.01 \mu\text{V}$ ; young–older: LSM =  $0.03 \mu\text{V}$ ,  $SE = 0.01 \mu\text{V}$ ) to a smaller extent than the IPM-FR amplitudes (young–middle-aged: LSM =  $0.07 \mu\text{V}$ ,  $SE = 0.02 \mu\text{V}$ ; young–older: LSM =  $0.09 \mu\text{V}$ ,  $SE = 0.02 \mu\text{V}$ ). These outcomes suggest that changes in IPM-FR amplitudes, rather than changes in EEG noise, determine how age and HI affect the overall signal-to-noise ratio of the neural responses. This was also confirmed by refitting the LME models for signal-to-noise ratio, that is, the mean IPM-FR response power divided by the mean power of the background noise, which revealed similar main and

interaction effects as the LME model with IPM-FR amplitudes as outcome measure.

### Behavioral IPD Discrimination Thresholds

Participants performed the behavioral IPD discrimination task three times. The geometric mean across three trials was used for further analyses, as test–retest reliability was good: The geometric root mean square of the within-subject *SDs* across three behavioral assessments was  $1^\circ$  for the young NH group (based on Plomp & Mimpfen, 1979). Figure 5 shows the geometric mean of the IPD discrimination thresholds and its geometric *SD* per participant group. Descriptive statistics are reported in Table 2. Please note that two participants, a middle-aged and older person with HI, were not able to perform the behavioral IPD discrimination task, that is, both participants indicated that they could not discriminate the dynamic from the static stimuli.

An independent factorial analysis of variance revealed a main effect of age on the behavioral IPD discrimination thresholds,  $F(2, 48) = 20.99$ ,  $p < .001$ , as is

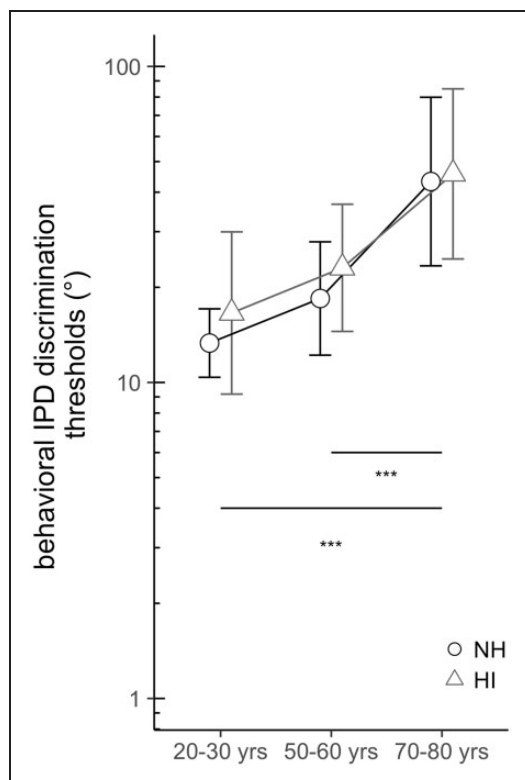


**Figure 5.** Behavioral IPD discrimination thresholds ( $^\circ$ ; y axis) as a function of age-group (x axis). Black circles and gray triangles represent geometric mean performances on the behavioral task for NH participants and participants with HI, respectively. Error bars visualize geometric standard deviations. \*\*\* $p$  values  $< .001$ . NH = normal hearing; HI = hearing impairment.

apparent from Figure 5 since IPD discrimination thresholds increase with advancing age. Bonferroni-corrected post hoc comparisons indicated that the behavioral thresholds were significantly higher (poorer discrimination) for older compared with middle-aged ( $p < .001$ ) and young participants ( $p < .001$ ). Young- and middle-aged participants performed equally well on the task ( $p = .13$ ). The independent factorial analysis of variance showed no main effect of hearing status,  $F(1, 48) = 1.48$ ,  $p = .23$ , as is apparent from the almost coinciding gray (HI) and black lines (NH) in Figure 5. The analyses did not reveal an interaction effect between hearing status and age either,  $F(2, 48) = 0.15$ ,  $p = .86$ .

### Relationship IPM-FR—Behavioral IPD Discrimination Thresholds

Spearman's rho correlation coefficients demonstrated that the dynamic range of the IPM-FR, that is, the difference between the maximum and minimum IPM-FR amplitude per participant, correlated with the behavioral IPD discrimination thresholds ( $r_s = -0.47$ ,  $p < .001$ ). This is illustrated by the scatterplot in Figure 6. A larger IPM-FR dynamic range was associated with lower (better) IPD discrimination. Both the IPM-FR dynamic range ( $r_s = -0.36$ ,  $p = .008$ ) and behavioral IPD discrimination thresholds ( $r_s = 0.65$ ,  $p < .001$ ) also correlated with age-group (young, middle-aged, and older). Partial Spearman's rho correlation coefficients, in turn, showed that, when age-group was corrected for, the behavioral IPD discrimination thresholds and

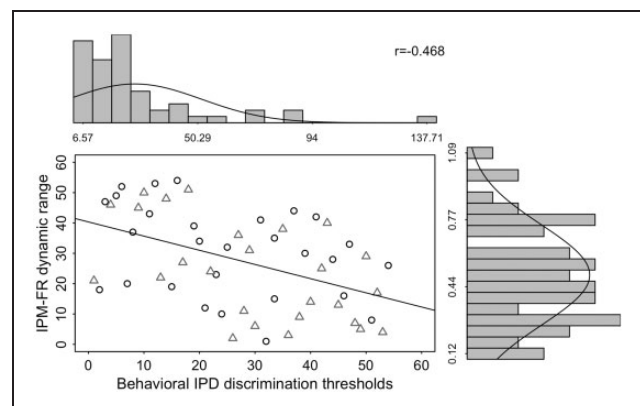


**Figure 6.** Scatterplot visualizing the ranks of the behavioral IPD discrimination thresholds (x axis) as a function of the ranks of the IPM-FR dynamic range (y axis). Black circles represent data of NH participants and gray triangles data of participants with HI. The histograms visualize the distributions of the raw data. The Spearman correlation coefficient is marked in the top right corner. IPM = interaural phase modulation; IPD = interaural phase difference.



the dynamic range of the IPM-FR were still significantly correlated ( $r_s = -0.33$ ,  $p = .02$ ).

### IPD Processing and Peripheral Hearing Sensitivity

Additional analyses were performed to determine whether or not age affected peripheral hearing sensitivity, despite the strict inclusion criteria. Across the HI cohorts, there was no effect of age on the hearing thresholds at 500 Hz,  $H(2) = 1.47$ ,  $p = .48$ . There was, however, an effect of age on the 500 Hz hearing thresholds for NH participants,  $H(2) = 11.75$ ,  $p = .003$ , with older participants having higher (poorer) hearing thresholds than young participants ( $U = 5$ ,  $z = -3.13$ ,  $p = .002$ ). It could be argued that these differences in peripheral hearing might have contributed to the changes in IPD processing that were revealed for older compared with young participants. Nonparametric spearman's rho correlations indeed confirmed the relationship between behavioral IPD discrimination thresholds and 500 Hz hearing threshold for NH participants ( $r_s = 0.63$ ,  $p < .001$ ). A partial spearman's rho, however, indicated that this relationship disappeared when age-group (young, middle-aged, and older) was controlled for ( $r_s = 0.29$ ,  $p = .14$ ). This suggests that the correlation between behavioral IPD processing and 500 Hz hearing thresholds is mediated by age and not by peripheral hearing.

### Discussion

This study aimed to disentangle potential contributions of age and HI to changes in binaural temporal processing in adult listeners. To this end, neural and behavioral IPD processing were investigated in young, middle-aged, and older participants with either NH or sensorineural HI.

Results showed that HI alters neural binaural processing in all age-groups, reflected by reduced amplitudes of the IPM-FRs. These HI-related changes set in, superimposed on age-related amplitude reductions that emerge between young adulthood and middle age. Poorer neural outcomes were also associated with poorer behavioral IPD discrimination thresholds. Age affected behavioral IPD processing, with reduced performance for older compared with young and middle-aged participants, whereas no effect of hearing status on the behavioral outcomes was revealed.

Our results demonstrate that age-related changes in IPM-FR amplitudes set in around the same time, that is, by middle-age, as morphological changes in cortical auditory evoked potentials elicited by changes in IPDs over time (Wambacq et al., 2009). Also the maximum carrier frequency for which IPDs evoke cortical auditory evoked potentials decreases by middle-age (Papesh et al., 2017; Ross et al., 2007). Do note that cortical auditory evoked potentials merely indicate a detection of change

(Clinard, Tremblay, & Krishnan, 2010), whereas the IPM-FRs extend our knowledge of the auditory system by quantifying the relative processing of different IPM depths (Haywood et al., 2015; McAlpine et al., 2016; Undurraga et al., 2016).

Superimposed on age-related changes, our results demonstrate that HI alters neural IPD processing for every age-group, even after a correction for stimulus audibility which simulates amplification through hearing aids. Interestingly, HI reduces neural responses to larger (suprathreshold) IPM depths more than to smaller IPM depths (near threshold; see Figure 4: gray and black linear fits dissociate above IPM depths of  $\pm 30^\circ$ ). Also, our behavioral data—which reflect IPD discrimination at threshold level—are in agreement with the neural data on how HI contributes less to threshold than to suprathreshold IPD processing (see Figure 5: IPD discrimination thresholds are similar for NH participants and participants with HI, independent of age cohort). By not revealing an effect of HI on behavioral IPD discrimination thresholds, our results are in line with other behavioral binaural outcomes (Eddins & Eddins, 2017; Hopkins & Moore, 2011; Lacher-Fougère & Demany, 2005; Moore et al., 2012; Strelcyk & Dau, 2009) and fall within the range of reference values (Hopkins & Moore, 2011). Overall, these results may reflect that only a few binaural neurons are required for detection tasks. Animal models and auditory nerve simulations have indeed showed that compound action potential thresholds shift little despite a high percentage of auditory nerve loss (Bourien et al., 2014; Salvi et al., 2017). To our knowledge, only King et al. (2014) showed an association between HI and behavioral IPD discrimination thresholds.

Across participant groups, correlation analyses did demonstrate a close correspondence between the IPM-FR dynamic range and behavioral IPD discrimination thresholds. These outcomes do suggest that similar mechanisms underlie the neural and behavioral measures of IPD processing and highlight the sensitivity of the IPM-FRs to detect changes in binaural temporal processing throughout adult life. In fact, the IPM-FRs could very well meet the need for a robust measure of binaural temporal processing that has long been lacking. The IPM-FRs could, for instance, contribute to evaluating binaural hearing aid fittings or assess changes in binaural temporal resolution in clinical settings. Do note that the IPM-FRs in this study measure binaural processing across a range of mainly suprathreshold IPM depths, whereas the behavioral measure reflects IPD processing at threshold level. This difference could have contributed to why the IPM-FRs demonstrate a susceptibility to age between young adulthood and middle age, whereas behavioral sensitivity deteriorates between middle-aged and older adults, as is consistent

with other behavioral studies (Grose & Mamo, 2010; Hopkins & Moore, 2011).

IPM-FRs presumably originate from neurons in cortical areas (Haywood et al., 2015; McAlpine et al., 2016; Undurraga et al., 2016). However, changes in IPM-FRs could also reflect reduced low-level temporal resolution. Both age and HI have indeed been associated with cochlear synaptic loss (Kujawa & Liberman, 2015) and progressive degeneration of spiral ganglion cells (Makary et al., 2011; McFadden et al., 2004; Spoendlin, 1975), reducing the temporal resolution on which TFS encoding relies (Bharadwaj, Verhulst, Shaheen, Liberman, & Shinn-Cunningham, 2014; Lopez-Poveda & Barrios, 2013). These forms of low-level neurodegeneration might affect later stages along the auditory pathway as well (Ozmeral, Eddins, & Eddins, 2016), even though they do not necessarily influence behavioral hearing thresholds (Kujawa & Liberman, 2009, 2015; Lobarinas, Salvi, & Ding, 2013; Schuknecht & Woellner, 1953). Changes in IPM-FRs could also reflect neurochemical changes in the central auditory pathway (King et al., 2014; Ozmeral et al., 2016). Reduced cochlear input toward the central auditory pathway—due to age or HI—is indeed associated with reduced neural inhibitory control (Caspary et al., 2008). These inhibitory changes are often referred to as a compensatory mechanism, as they are associated with increased cortical activity, that is, central gain, in animal models (Chambers et al., 2016; Salvi et al., 2017). Interestingly, we recently demonstrated that advancing age yields increased neural excitability at cortical level in human listeners as well (Goossens et al., 2016). The neural activity was evoked by unilateral and bilateral low-frequency (~4 Hz) envelope modulations in similar participants as were recruited for this study. It is likely that the underlying mechanisms of central gain also affect IPD processing. Not only is precisely timed inhibitory control crucial for the encoding of interaural delays (Brand, Behrend, Marquardt, McAlpine, & Grothe, 2002; Pecka, Brand, Behrend, & Grothe, 2008), the increased spontaneous activity that is associated with changes in inhibitory control (Caspary et al., 2008) could very well increase the amount of jitter on binaural neural transmission, thereby reducing phase locking in binaural cells.

Altogether, this study is the first to disentangle contributions of age and HI to changes in binaural temporal processing in adult listeners. The neural outcomes demonstrate a dual load that could pose great challenges on binaural hearing in daily life and, as such, they suggest looking into the possibility of binaural training. In addition, the association between the neural and behavioral outcomes illustrates the sensitivity of the IPM-FRs to detect changes in binaural temporal resolution, thereby

possibly meeting the need for a robust measure that has long been lacking.

### Acknowledgments

The authors would like to thank all participants who participated in this study and Marianne Blokken, Catriona Byl, Caroline Storms, and Loes Wynants for their help in collecting the data.


### Declaration of Conflicting Interests

The author(s) declared no potential conflicts of interest with respect to the research, authorship, and/or publication of this article.

### Funding

The author(s) disclosed receipt of the following financial support for the research, authorship, and/or publication of this article: This work was supported by the Research Council of KU Leuven (grant support: OT/12/98), the Research Foundation—Flanders (Fonds voor Wetenschappelijk Onderzoek [FWO]) through an FWO-aspirant grant to Tine Goossens (grant number: 11Z8817N), and the Australian Government through the Australian Research Council (project number: FL160100108).

### ORCID iD

Charlotte Vercammen  <http://orcid.org/0000-0002-4517-6910>

### References

- American Clinical Neurophysiology Society. (2006). Guideline 5: Guidelines for standard electrode position nomenclature. *American Journal of Electroneurodiagnostic Technology*, 46(3), 222–225. doi:10.1080/1086508X.2006.11079580
- Baayen, R. H., Davidson, D. J., & Bates, D. M. (2008). Mixed-effects modeling with crossed random effects for subjects and items. *Journal of Memory and Language*, 59(4), 390–412. doi:10.1016/j.jml.2007.12.005
- Bates, D., Machler, M., Bolker, B. M., & Walker, S. C. (2015). Fitting linear mixed-effects models using lme4. *Journal of Statistical Software*, 67, 1–51. doi:10.18637/jss.v067.i01
- Bharadwaj, H. M., Verhulst, S., Shaheen, L., Liberman, M. C., & Shinn-Cunningham, B. G. (2014). Cochlear neuropathy and the coding of supra-threshold sound. *Frontiers in Systems Neuroscience*, 8, 1–18. doi:10.3389/fnsys.2014.00026
- Bourien, J., Tang, Y., Batrel, C., Huet, A., Lenoir, M., Ladrech, S., . . . Wang, J. (2014). Contribution of auditory nerve fibers to compound action potential of the auditory nerve. *Journal of Neurophysiology*, 112(5), 1025–1039. doi:10.1152/jn.00738.2013
- Brand, A., Behrend, O., Marquardt, T., McAlpine, D., & Grothe, B. (2002). Precise inhibition is essential for micro-second interaural time difference coding. *Nature*, 417(6888), 543–547. doi:10.1038/417543a
- Carhart, R., & Jerger, J. (1959). Preferred method for clinical determination of pure-tone thresholds. *Journal of Speech & Hearing Disorders*, 24, 330–345. doi:10.1044/jshd.2404.330

- Caspary, D. M., Ling, L., Turner, J. G., & Hughes, L. F. (2008). Inhibitory neurotransmission, plasticity and aging in the mammalian central auditory system. *The Journal of Experimental Biology*, *211*, 1781–1791. doi:10.1242/jeb.013581
- CHABA. (1988). Speech understanding and aging. *The Journal of the Acoustical Society of America*, *83*(3), 859–895. doi:10.1121/1.395965
- Chambers, A. R., Resnik, J., Yuan, Y., Whitton, J. P., Edge, A. S., Liberman, M. C., & Polley, D. B. (2016). Central gain restores auditory processing following near-complete cochlear denervation. *Neuron*, *89*(4), 867–879. doi:10.1016/j.neuron.2015.12.041
- Clinard, C. G., Tremblay, K. L., & Krishnan, A. R. (2010). Aging alters the perception and physiological representation of frequency: Evidence from human frequency-following response recordings. *Hearing Research*, *264*, 48–55. doi:10.1016/j.heares.2009.11.010
- Eddins, A. C., & Eddins, D. A. (2018). Cortical correlates of binaural temporal processing deficits in older adults. *Ear and Hearing*, *39*(3), 594–604.
- Francart, T., van Wieringen, A., & Wouters, J. (2008). APEX 3: A multi-purpose test platform for auditory psychophysical experiments. *Journal of Neuroscience Methods*, *172*(2), 283–293. doi:10.1016/j.jneumeth.2008.04.020
- Füllgrabe, C. (2013). Age-dependent changes in temporal-fine-structure processing in the absence of peripheral hearing loss. *American Journal of Audiology*, *22*(2), 313–315. doi:10.1044/1059-0889(2013/12-0070)
- Gates, G., & Mills, J. (2005). Presbycusis. *The Lancet*, *366*, 1111–1120. doi:10.1016/S0140-6736(05)67423-5
- Goossens, T., Vercammen, C., Wouters, J., & van Wieringen, A. (2016). Aging affects neural synchronization to speech-related acoustic modulations. *Frontiers in Aging Neuroscience*, *8*, 1–23. doi:10.3389/fnagi.2016.00133
- Gransier, R., van Wieringen, A., & Wouters, J. (2017). Binaural interaction effects of 30–50 Hz auditory steady-state responses. *Ear and Hearing*, *38*(5), e305–e315. doi:10.1097/AUD.0000000000000429
- Große, J. H., & Mamo, S. K. (2010). Processing of temporal fine structure as a function of age. *Ear and Hearing*, *31*(6), 755–760. doi:10.1097/AUD.0b013e3181e627e7
- Haywood, N. R., Undurraga, J. A., Marquardt, T., & McAlpine, D. (2015). A comparison of two objective measures of binaural processing. *Trends in Hearing*, *19*, 1–17. doi:10.1177/2331216515619039
- Heil, P., & Peterson, A. J. (2015). Basic response properties of auditory nerve fibers: A review. *Cell and Tissue Research*, *361*, 129–158. doi:10.1007/s00441-015-2177-9
- Hopkins, K., & Moore, B. C. J. (2011). The effects of age and cochlear hearing loss on temporal fine structure sensitivity, frequency selectivity, and speech reception in noise. *The Journal of the Acoustical Society of America*, *130*(1), 334–349. doi:10.1121/1.3585848
- IBM Corporation. (2016). *IBM SPSS statistics for Windows (Version 24.0) [Computer software]*. Armonk, NY: Author.
- King, A., Hopkins, K., & Plack, C. J. (2014). The effects of age and hearing loss on interaural phase difference discrimination. *The Journal of the Acoustical Society of America*, *135*(1), 342–351. doi:10.1121/1.4838995
- Koerner, T. K., & Zhang, Y. (2017). Application of linear mixed-effects models in human neuroscience research: A comparison with Pearson correlation in two auditory electrophysiology studies. *Brain Sciences*, *7*(3), 1–11. doi:10.3390/brainsci7030026
- Kujawa, S. G., & Liberman, M. C. (2009). Adding insult to injure: Cochlear nerve degeneration after ‘temporary’ noise-induced hearing loss. *The Journal of Neuroscience*, *29*(45), 14077–14085. doi:10.1523/JNEUROSCI.2845-09.2009
- Kujawa, S. G., & Liberman, M. C. (2015). Synaptopathy in the noise-exposed and aging cochlea: Primary neural degeneration in acquired sensorineural hearing loss. *Hearing Research*, *330*, 191–199. doi:10.1016/j.heares.2015.02.009
- Kuznetsova, A., Brockhoff, P. B., & Christensen, R. H. B. (2016). lmerTest: Tests in linear mixed effects models. Retrieved from <https://cran.r-project.org/package=lmerTest>
- Lacher-Fougère, S., & Demany, L. (2005). Consequences of cochlear damage for the detection of interaural phase differences. *The Journal of the Acoustical Society of America*, *118*(4), 2519–2526. doi:10.1121/1.2032747
- Levitt, H. (1971). Transformed up-down methods in psychoacoustics. *The Journal of the Acoustical Society of America*, *49*, 467–477. doi:10.1121/1.1912375
- Lister, J. J., Harrison Bush, A. L., Ansel, R., Matthews, C., Morgan, D., & Edwards, J. D. (2016). Cortical auditory evoked responses of older adults with and without probable mild cognitive impairment. *Clinical Neurophysiology*, *127*(2), 1279–1287. doi:10.1016/j.clinph.2015.11.007
- Lobarinas, E., Salvi, R., & Ding, D. (2013). Insensitivity of the audiogram to carboplatin induced inner hair cell loss in chinchillas. *Hearing Research*, *302*, 113–120. doi:10.1016/j.heares.2013.03.012
- Lopez-Poveda, E. A., & Barrios, P. (2013). Perception of stochastically undersampled sound waveforms: A model of auditory deafferentation. *Frontiers in Neuroscience*, *7*, 1–13. doi:10.3389/fnins.2013.00124
- McAlpine, D., Haywood, N., Undurraga, J., & Marquardt, T. (2016). Objective measures of neural processing of interaural time differences. *Advances in Experimental Medicine and Biology*, *894*, 197–205. doi:10.1007/978-3-319-25474-6
- McFadden, S. L., Ding, D., Jiang, H., & Salvi, R. J. (2004). Time course of efferent fiber and spiral ganglion cell degeneration following complete hair cell loss in the chinchilla. *Brain Research*, *997*, 40–51. doi:10.1016/j.brainres.2003.10.031
- Magezi, D. A. (2015). Linear mixed-effects models for within-participant psychology experiments: An introductory tutorial and free, graphical user interface (LMMgui). *Frontiers in Psychology*, *6*, 1–7. doi:10.3389/fpsyg.2015.00002
- Makary, C. A., Shin, J., Kujawa, S. G., Liberman, M. C., & Merchant, S. N. (2011). Age-related primary cochlear neuronal degeneration in human temporal bones. *Journal of the Association for Research in Otolaryngology*, *12*, 711–717. doi:10.1007/s10162-011-0283-2
- Moore, B. C. J. (2014). *Auditory processing of temporal fine structure: Effects of age and hearing loss*. Singapore: World Scientific Publishing.
- Moore, B. C. J., Glasberg, B. R., Stoev, M., Füllgrabe, C., & Hopkins, K. (2012). The influence of age and high-frequency hearing loss on sensitivity to temporal fine structure

- at low frequencies (L). *The Journal of the Acoustical Society of America*, 131(2), 1003–1006. doi:10.1121/1.3672808.
- Nasreddine, Z. S., Phillips, N. A., Bédirian, V., Charbonneau, S., Whitehead, V., Collin, I., . . . Chertkow, H. (2005). The Montreal Cognitive Assessment, MoCA: A brief screening tool for mild cognitive impairment. *Journal of the American Geriatrics Society*, 53, 695–699. doi:10.1111/j.1532-5415.2005.53221.x.
- Oberfeld, D., & Klöckner-Nowotny, F. (2016). Individual differences in selective attention predict speech identification at a cocktail party. *eLIFE*, 5(e16747), 1–24. doi:10.7554/eLife.16747.
- Ozmeral, E. J., Eddins, D. A., & Eddins, A. C. (2016). Reduced temporal processing in older normal-hearing listeners evident from electrophysiological responses to shifts in interaural time difference. *Journal of Neurophysiology*, 116(6), 2720–2729. doi:10.1152/jn.00560.2016.
- Papesh, M. A., Folmer, R. L., & Gallun, F. J. (2017). Cortical measures of binaural processing predict spatial release from masking performance. *Frontiers in Human Neuroscience*, 11(124), 1–15. doi:10.3389/fnhum.2017.00124.
- Pecka, M., Brand, A., Behrend, O., & Grothe, B. (2008). Interaural time difference processing in the mammalian medial superior olive: The role of glycinergic inhibition. *The Journal of Neuroscience*, 28(27), 6914–6925. doi:10.1523/JNEUROSCI.1660-08.2008.
- Plomp, R., & Mimpen, A. M. (1979). Improving the reliability of testing the speech reception threshold for sentences. *International Journal of Audiology*, 18(1), 43–52. doi:10.3109/00206097909072618.
- R Core Team. (2017). R: A language and environment for statistical computing [Computer software]. Vienna, Austria: R Foundation for Statistical Computing. Retrieved from <https://www.r-project.org/>.
- Remme, M. W. H., Donato, R., Mikiel-Hunter, J., Ballester, J. A., Foster, S., Rinzel, J., & McAlpine, D. (2014). Subthreshold resonance properties contribute to the efficient coding of auditory spatial cues. *Proceedings of the National Academy of Sciences of the United States of America*, 111(22), E2339–E2348. doi:10.1073/pnas.1316216111.
- Rose, J. E., Brugge, J. F., Anderson, D. J., & Hind, J. E. (1967). Phase-locked response to low-frequency tones in single auditory nerve fibers of the squirrel monkey. *Journal of Neurophysiology*, 30(4), 769–793. doi:10.1152/jn.1967.30.4.769.
- Ross, B., Fujioka, T., Tremblay, K. L., & Picton, T. W. (2007). Aging in binaural hearing begins in mid-life: Evidence from cortical auditory-evoked responses to changes in interaural phase. *The Journal of Neuroscience*, 27(42), 11172–11178. doi:10.1523/JNEUROSCI.1813-07.2007.
- Salvi, R., Sun, W., Ding, D., Chen, G.-D., Lobarinas, E., Wang, J., . . . Auerbach, B. D. (2017). Inner hair cell loss disrupts hearing and cochlear function leading to sensory deprivation and enhanced central auditory gain. *Frontiers in Neuroscience*, 10, 1–14. doi:10.3389/fnins.2016.00621.
- Schuknecht, H. F., & Woellner, R. C. (1953). Hearing losses following partial section of the cochlear nerve. *The Laryngoscope*, 63(6), 441–465. doi:10.1288/00005537-195306000-00001.
- Sergeyenko, Y., Lall, K., Liberman, M. C., & Kujawa, S. G. (2013). Age-related cochlear synaptopathy: An early-onset contributor to auditory functional decline. *The Journal of Neuroscience*, 33(34), 13686–13694. doi:10.1523/JNEUROSCI.1783-13.2013.
- Spoendlin, H. (1975). Factors inducing retrograde degeneration of the cochlear nerve. *Acta Oto-Laryngologica*, 79, 266–275. doi:10.3109/00016487509124683.
- Strelcyk, O., & Dau, T. (2009). Relations between frequency selectivity, temporal fine-structure processing, and speech reception in impaired hearing. *The Journal of the Acoustical Society of America*, 125(5), 3328–3345. doi:10.1121/1.3097469.
- Swaminathan, J., & Heinz, M. G. (2012). Psychophysiological analyses demonstrate the importance of neural envelope coding for speech perception in noise. *The Journal of Neuroscience*, 32(5), 1747–1756. doi:10.1523/JNEUROSCI.4493-11.2012.
- Swaminathan, J., Mason, C. R., Streeter, T. M., Best, V., Roverud, E., & Kidd, G. (2016). Role of binaural temporal fine structure and envelope cues in cocktail-party listening. *The Journal of Neuroscience*, 36(31), 8250–8257. doi:10.1523/JNEUROSCI.4421-15.2016.
- Tremblay, K., Picton, T. W., & Ross, B. (2007). Auditory evoked MEG responses to interaural phase changes: Effects of aging on response latencies. *International Congress Series*, 1300, 69–72. doi:10.1016/j.ics.2007.01.057.
- Undurraga, J. A., Haywood, N. R., Marquardt, T., & McAlpine, D. (2016). Neural representation of interaural time differences in humans—An objective measure that matches behavioural performance. *Journal of the Association for Research in Otolaryngology*, 17(6), 591–607. doi:10.1007/s10162-016-0584-6.
- Wambacq, I. J. A., Koehnke, J., Besing, J., Romei, L. L., DePierro, A., & Cooper, D. (2009). Processing interaural cues in sound segregation by young and middle-aged brains. *Journal of the American Academy of Audiology*, 20(7), 453–459. doi:10.3766/jaaa.20.7.6.
- Zeng, F.-G., Nie, K., Stickney, G. S., Kong, Y.-Y., Vongphoe, M., Bhargava, A., . . . Cao, K. (2005). Speech recognition with amplitude and frequency modulations. *Proceedings of the National Academy of Sciences of the United States of America*, 102(7), 2293–2298. doi:10.1073/pnas.0406460102.